Datum
2024-09-09

Dnr
P2021-00011

Projektnr
P112580

Energimyndighetens titel på projektet – svenska Utveckling av Billiga Zeoliter för Kostnadseffektiv Koldioxidavskiljning	
Energimyndighetens titel på projektet – engelska Development of Low-Cost Zeolites for Cost-Efficient CO_2 Capture	
Universitet/högskola/företag RISE Research Institutes of Sweden AB	Avdelning/institution Infrastruktur och Betongbyggande
Adress Gibraltargatan 35, 41279 Göteborg	
Namn på projektledare Anders Höije	
Namn på ev övriga projektdeltagare Placid Atongka Tchoffor Henrik Leion Marcus Hedberg Jonas Zetterholm Anton Coates Christian Olausson Björn Haase Ulf Börner Oscar Lyttbacka	
Nyckelord: 5-7 st CCS, zeolit, koldioxidavskiljning, restprodukter, adsorption	

Box 310 • 631 04 Eskilstuna • Besöksadress Kungsgatan 43
Telefon 016-544 20 00 • Telefax 016-544 20 99
registrator@energimyndigheten.se
www.energimyndigheten.se
Org.nr 202100-5000

Förord

Detta projekt har kunnat genomföras tack vara ekonomiskt stöd från Energimyndigheten genom programmet Industriklivet samt från deltagande industripartners; Höganäs Sweden AB, Lidköping Energi AB, Zeo Concept ECE AB och HaloSep AB. Referensgruppen, som har bestått av nyckelpersoner från samtliga industripartners samt från Chalmers och RISE, har bidragit stort till projektets framgång genom sin kompetens, engagemang och värdefulla diskussioner. Stort tack till alla inblandade.

Table of contents

Sammanfattning

Avskiljning och lagring av koldioxid (CCS) är nödvändigt för att Sverige ska uppfylla sitt mål om noll nettoutsläpp av växthusgaser till 2045. CO_2-separering står för 70–80 % av den totala CCS-kostnaden där CO_2-separeringsmaterialet står för den största kostnaden. I detta projekt har RISE, Chalmers och ett antal industriella partners utvecklat en kostnadseffektiv CO_2-separering baserad på zeoliter framställda av industrirester. OPEX för produktionen av zeoliter varierar beroende på råvaror och ger olika prisscenarier från 0,3 till 2,6 EUR/kg. Råvaror som cyklon aska och Petrit L ger de bästa resultaten och kostnaden för NaOH och HCl är de primära kostnadsdrivarna. Även om de nuvarande OPEX-siffrorna är lovande, särskilt för vissa råvaror, finns det potential för ytterligare minskning genom optimering av kemikalieanvändningen. Ytterligare kostnadsfaktorer som råvaruhantering, intäkter från avfallsanvändning, kapitalkostnader och CO_2-avskiljningsprestanda tas dock inte med i denna analys och kan väsentligt påverka processens tekniska ekonomiska livskraft.

Summary

Carbon capture and storage (CCS) is necessary for Sweden to reach zero net greenhouse gas emissions by 2045. CO_2 separation accounts for 70%–80% of the total CCS cost with the CO_2 separation material being the main cost contributor. In this project RISE, Chalmers and industrial partners have developed cost-efficient CO_2 separation based on zeolites produced from industrial residues as starting feedstocks. OPEX for producing the zeolites varies depending on feedstocks and price scenarios, ranging from 0.3 to 2.6 EUR/kg. Feedstocks like Cyclone ash and Petrit L yield the best results and cost for NaOH and HCl are the primary cost drivers. While the current OPEX figures are promising, especially for certain feedstocks, there is potential for further reduction through the optimisation of chemical usage. However, additional cost factors such as feedstock handling, income from waste utilisation, capital costs, and CO_2 capture performance are not accounted for in this analysis and could significantly affect the techno-economic viability of the process.

Introduction/Background

Introduction: The emission of greenhouse gases from process industries accounted for 32 % of Sweden's territorial greenhouse gas emissions (50.9 M tonnes CO_2-equivalent) for the year 2019. To contribute to Sweden's goal to reach net-zero greenhouse gas emissions by 2045, process industries such as the cement industry and steel industry have identified CCS (including BEECS) in their respective roadmaps ("Färdplan Cement för ett Klimatneutral Betongbyggande;[1] Klimatfärdplan för en Fossilfri och Konkurrenskraftig Stålindustri I Sverige[2]) as an important measure that can help them to reach climate neutrality.

Conventional CCS consists of 3 main steps, namely separation of CO_2 from flue gases, transportation and storage in suitable geological sites such as depleted oil and gas reservoirs.[3] The total CCS cost for a wide range of industries in Sweden has been estimated to be ~1000 SEK/tonne of CO_2 sequestered.[4] This is significantly higher than the current price for CO_2 emission permit which is about 500-800 SEK/tonne of CO_2 emitted.[5] Generally, the separation of CO_2 from flue gases accounts for 70–80 % of the total CCS cost wherein the main items driving up cost are the CO_2 separation efficiency and cost of the material applied for CO_2 separation.[6] [7]Thus, the development of cost-efficient CO_2 separation materials is crucial for the economic viability of CCS.[8] Chemical absorption based on monoethanolamine (MEA) scrubbing is currently the benchmark for CO_2 separation.[9-11] However, the regeneration of MEA is energy-intensive (it consumes 3–6 GJ/tonne of captured CO_2)[8, 12, 13] and thus results in a significant reduction in the performance of the plant in which it is applied. As an example, a recent (year 2020) study carried out at Karlstad Energi AB revealed that the implementation of MEA for CO_2 separation in its CHP plant will result in drastic reductions in the production of electricity and heat in the order of 65–87 % and 66–86 % respectively.[14] Energy consumption in the range ≤ 2 GJ/tonne of CO_2 is deemed necessary to significantly reduce the cost of CO_2 capture, and thus make CCS more economically viable for industries.[15] The intense-heat regeneration of MEA combined with other disadvantages notably hazardous substances resulting from its degradation makes MEA not economically and environmentally viable for industries.[7] Thus, alternative processes and materials for CO_2 separation are under development among which physical adsorption with zeolites is considered to be promising.[9] Zeolites are crystalline microporous aluminosilicate minerals that have pore sizes typically between 4 and 15 Å, and surface areas around 200–700 m^2/g.[16, 17] They combine high adsorption capacities at ambient pressure with high thermal stability reaching up to 600°C.[18] The most common zeolite used for CO_2 separation is zeolite 13 X. Its heat of regeneration in pilot plant studies[7, 19] has been estimated to be in the range 0.65–2.0 GJ/tonne captured CO_2 which is significantly lower than the 3–6 GJ/tonne of captured CO_2 for MEA. The main barrier to the industrial deployment of zeolites for CO_2 separation is its high cost. Commercial zeolite 13 X is synthesized from chemical reagent-grade sources of alumina and silica which are expensive. In fact, the price for zeolite 13 X with pore openings of size 0.3–0.4 nm that are suitable for CO_2 capture lies in the range 1800–3000 SEK/kg (Sigma Aldrich 2024-05-28).

Background: To enable the industrial deployment of zeolites for CO_2 separation in an economically viable manner, global research is currently focused on the development of cost-efficient zeolitic sorbents from low-cost feedstocks such as industrial residues and natural zeolites.[20, 21] For example, zeolite 13 X produced from coal fly ash was observed to have a higher surface area (643 m^2/g) than that of commercial zeolite 13 X (595 m^2/g).[22] Under similar experimental conditions, the produced zeolite was observed to have a higher CO_2 adsorption capacity (225 mg of CO_2/g of zeolite) compared to commercial zeolite 13X (190 g of CO_2/kg of zeolite).[22] Examples of low-cost feedstocks in Sweden that could be used as starting feedstocks for zeolite production are Si and Al-rich industrial residues such as metallurgical slags, boiler ash, and mine tailings. Thousands of tons of metallurgical slags and boiler ash are produced in Sweden annually some of which are landfilled. Cost-efficient zeolites for CO_2 separation can also be produced through the modification of low-cost natural zeolites.[21] Examples of natural zeolites that can be used here are clinoptilolite, chabazite, and erionite.[21]

Aim: The aim of this study is to develop low-cost zeolitic sorbents from industrial residues and natural zeolites for CO_2 separation.
To meet the aim of the project, the following objectives are defined:

1. Develop zeolitic sorbents from industrial residues and natural zeolites with comparable CO_2 separation properties as commercial zeolite 13X. Notably with CO_2 working capacities close or higher than that (60–190 g of CO_2 per kg of zeolite 13X)[22-24] of commercial zeolite 13X.
2. Evaluate the CO_2 separation performance of the developed sorbents in simulated flue gases containing CO_2 of various concentrations.
3. Preliminary estimate of the cost to produce the sorbents.

Theory

Physical adsorption is emerging as a cost-efficient alternative technology for post-combustion CO_2 separation compared to chemical scrubbing with MEA which is the current benchmark.[25] Post-combustion CO_2 separation by physical adsorption is carried out in a cyclic process which consists of two main steps namely adsorption and desorption, see Figure 1. In the adsorption step, CO_2 is adsorbed on the applied solid sorbent, and thus is separated from the other components in the flue gas (e.g., N_2, SO_2, etc). In the desorption step, the adsorbed CO_2 is desorbed from the sorbent and recovered, leading to the regeneration of the sorbent. CO_2 separation by physical adsorption is carried through three main processes namely temperature swing adsorption (TSA), pressure swing adsorption (PSA), and vacuum swing adsorption (VSA). In TSA, the adsorbed CO_2 is desorbed from the adsorbent by heating the adsorbent with a hot gas or steam.[26] In PSA, adsorption of CO_2 on the adsorbent is generally carried out at pressures higher than atmospheric pressure while the desorption of CO_2 from the adsorbent is generally carried out at atmospheric pressure.[26] In VSA, adsorption on CO_2 on the adsorbent is carried out at atmospheric pressure and near-room temperature

while desorption of CO_2 from the sorbent is carried out at pressures lower than atmospheric pressure.[26]

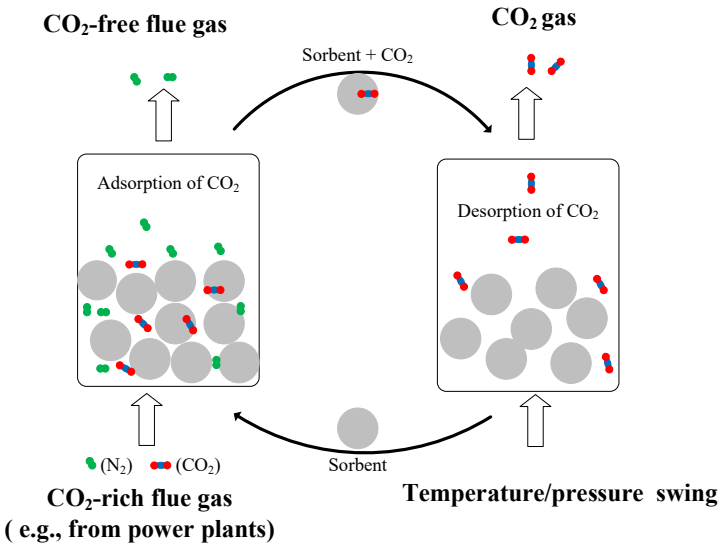

Figure 1. Schematic of a CO_2 separation process by physical adsorption.

To enhance the technoeconomic viability of CO_2 separation by physical adsorption, combinations of two of these main processes could also be applied, e.g., vacuum-pressure swing adsorption (VPSA), temperature-vacuum swing adsorption (TVSA) and pressure-temperature swing adsorption (PTSA).[27, 28] For example, Jiang et al compared the performances of the TSA, TVSA , and VPSA methods for CO_2 separation by physical adsorption. In terms of energy consumption, they found out that the VPSA process required the least amount of energy per kg of separated CO_2 as shown in the Figure 2. For the sake of simplicity, only the TSA will be applied in this study to evaluate the performance of the developed sorbents for CO_2 separation.

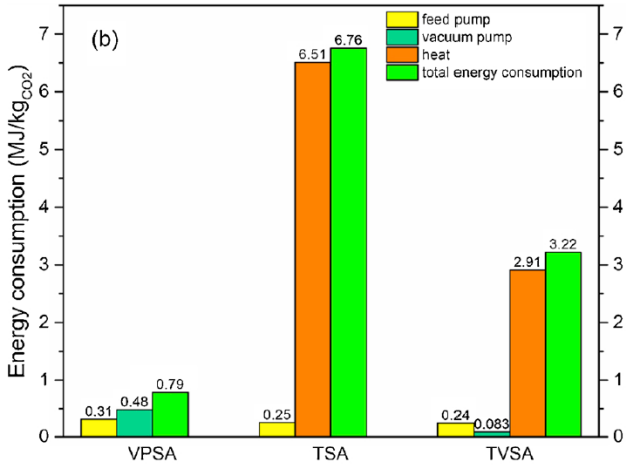

Figure 2. Energy consumption for CO_2 separation in TSA, TVSA, and VPSA processes.

Some properties of a good sorbent for CO_2 separation by physical adsorption are:

i. High CO_2 working capacity: The CO_2 working capacity is defined as the difference in the quantity of CO_2 adsorbed during the adsorption and desorption stages of each CO_2 adsorption-CO_2 desorption cycle.[23, 25, 29] It determines the quantity of sorbent and therefore the reactor volume needed for CO_2 capture–thus impacting the capital cost of the CO_2 capture plant.[30] A sorbent with a high CO_2 working capacity reduces the amount of sorbent needed and consequently the size of reactor and capital cost for the CO_2 capture plant. According to Ho et al,[31] a solid sorbent with a CO_2 working capacity of 189.2 g of CO_2 per kg sorbent and a CO_2 selectivity over N_2 of 150 can result in a CO_2 separation cost that is < US$30 per tonne of CO_2 avoided–which is much lower than that (US$49 per tonne of CO_2 avoided) of MEA.

ii. High CO_2 selectivity: A high selectivity of CO_2 over other gases in the flue gas reduces transportation and storage or utilization costs.[25]

iii. High stability and recyclability: To reduce operational cost, a good sorbent should have thermochemical stability (and thus a long life span) as it alternates between the adsorption and desorption stages during CO_2 separation. The sorbent should be able to be used for many adsorption-desorption cycles.

iv. Low-cost: A low-cost sorbent reduced the operational cost of the CO_2 capture process. A sorbent cost ~ US$5 of is recommended to an economically viable CO_2 capture plant.[30] In comparison, the cost of commercial zeolite 13 X which is the benchmark sorbent for CO_2 separation by physical adsorbent is ~1000–3000 SEK/kg. There is thus a need to develop low-cost sorbents for CO_2 separation.

v. Low energy consumption: Energy consumption to for regenerating the sorbent during CO_2 separation should be as low as possible (lower than that of MEA).[25]

Material and Method

Feedstocks: The feedstocks used in the project were boiler ash fractions, namely filter ash (denoted FA) and cyclone ash (denoted CA), pretreated ash (denoted HS), metallurgical slag, namely tunnel kiln lime (denoted PL), and natural zeolite, namely Clinoptilolite (denoted NZ). The boiler ash fractions were supplied by Lidköping Energi AB, the pretreated ash was supplied by HaloSep AB, the metallurgical slag was supplied by Höganäs Sweden AB, and the natural zeolite was supplied by Zeo-Concept AB. Pure chemicals namely sodium hydroxide (NaOH), sodium aluminate ($NaAlO_2$) and hydrochloric acid (HCl) needed for the preparation of the zeolites were purchased from Fisher Scientific. Commercial zeolite 13X (benchmark adsorbent for CO_2 separation) was purchased from Fisher Scientific. The elemental compositions of the feedstocks are shown in Figure 3.

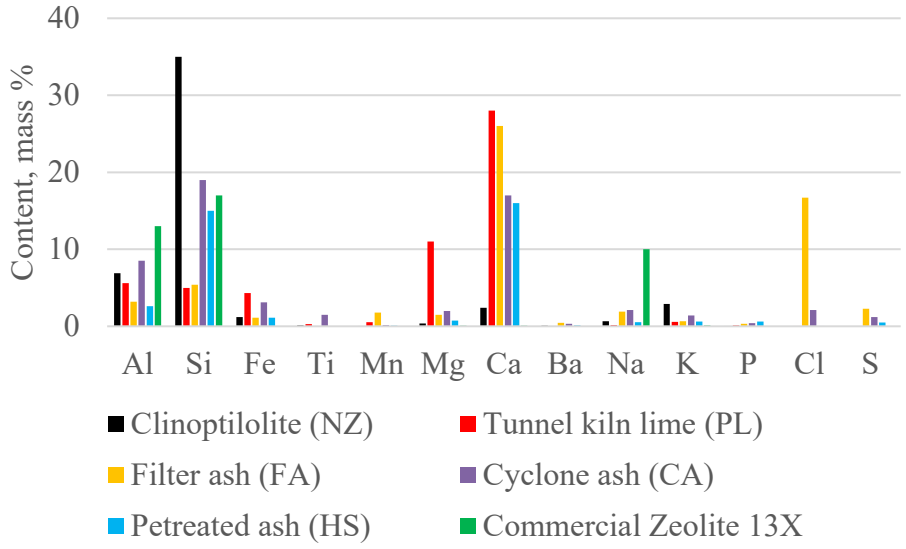

Figure 3. Elemental composition of feedstocks as well as commercial zeolite 13X.

Synthesis of zeolites from the feedstocks: A schematic of the process applied to produce zeolites from the feedstocks is shown in Figure 4. A detailed description of the process is available in Appendix 1 and Appendix 2. Briefly described, the process consisted of three main steps namely leaching, alkali fusion, and hydrothermal synthesis. In the leaching step, calcium and other inorganic impurities in the applied feedstocks were leached out at 80°C with a 1.5 M solution of HCl acid. The solid residue obtained from the leaching step was properly rinsed with deionized water and dried to constant mass in an oven. In the alkali fusion step, the dried solid residue was mixed with solid NaOH and heated in a muffle furnace at 500°C for 1 hour. In the hydrothermal synthesis step, the fused solid was mixed with deionized water and heated at 70°C or 90°C. In some of the experiments, the Al content of the solid residue was increased by adding $NaAlO_2$ (see sorbents CA-2 and NZ-2 in Table 1) prior to the hydrothermal synthesis reaction. Thereafter, the product was filtered, and rinsed with deionized water, and dried in an oven to constant mass.

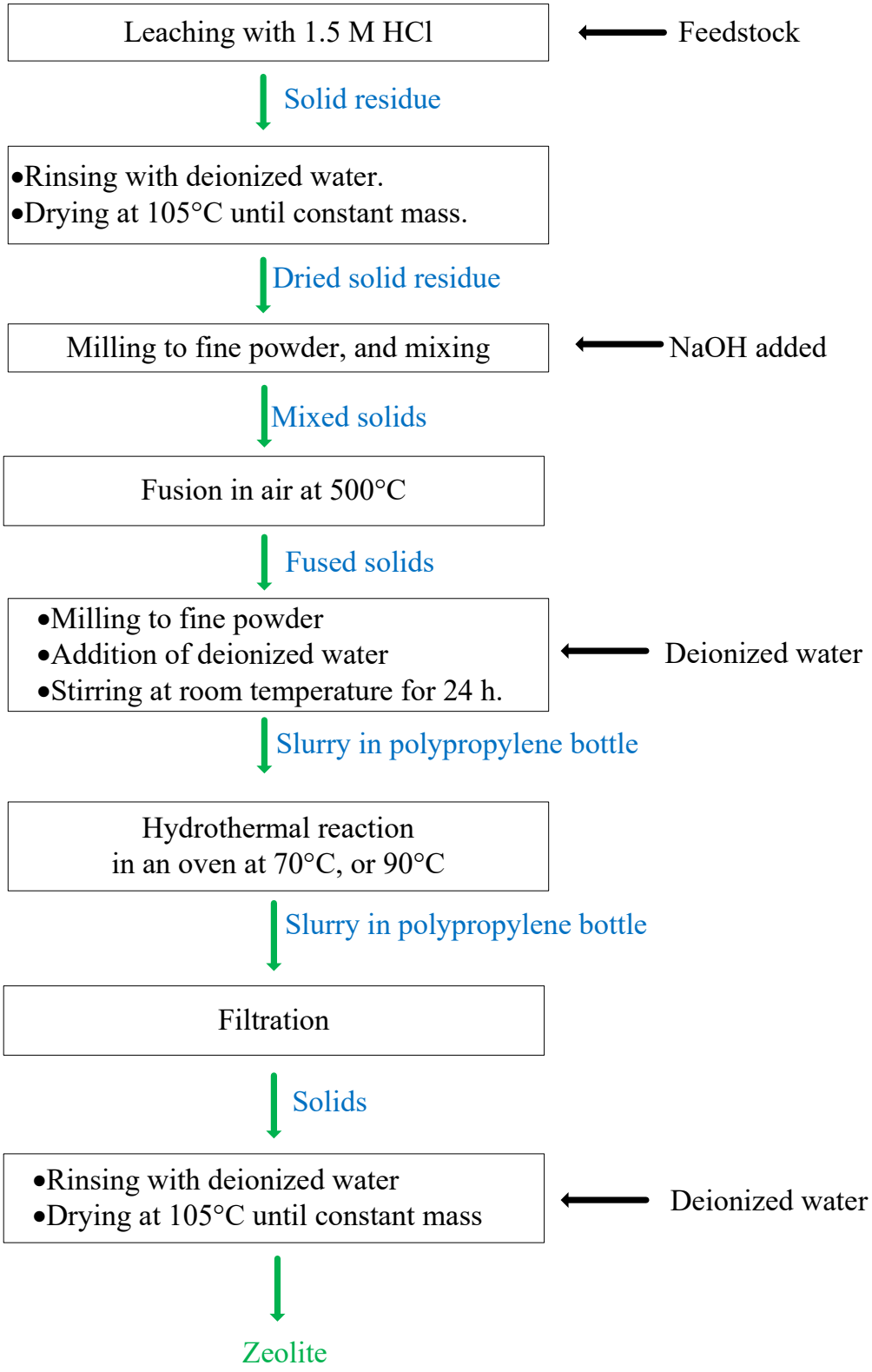

Figure 4. Steps taken to developed zeolitic sorbents form the applied feedstocks.

Physiochemical characterization of the produced zeolites: This was carried out with techniques such as powder XRD (x-ray diffraction; for identification of crystalline phases), specific surface area analysis (BET - Brunaure Emmet Teller model), and XRF (X-ray Fluorescence; for elemental composition).

Evaluation of CO_2 adsorption performance: The CO_2 working capacities of the developed sorbents were evaluated with the temperature swing adsorption technique using a thermogravimetric analyzer (Mettler Toledo TGA 1). Simulated flue gas compositions consisting of 15 % CO_2 in N_2 gas (reflects CO_2 concentration in the flue gas from heat and power plants), and 40 % CO_2 in N_2 gas (reflects CO_2 concentration in industrial chemical transformation processes) were used. Furthermore, 100 % CO_2 gas was also used to determine the maximum CO_2 adsorption capacity of the produced sorbents. 100 % N_2 gas was applied to give an indication of the CO_2 selectivity of the developed sorbents.

CO_2 adsorption and desorption experiments were carried out as follows:

i. Adsorption: 3–5 mg of a given sorbent was placed in a weighed crucible and placed in the TGA instrument. The sorbent was heated from room temperature to 200°C in nitrogen gas and held under this condition for 30 minutes to degas the sorbent. Thereafter, the sorbent was cooled in the chosen CO_2 gas mixture from 200°C to 25 °C or 35°C–the desired CO_2 adsorption temperatures. Initially, the sorbent was cooled in 100 % N_2 gas but it was later observed that the sorbent adsorbed some N_2 gas during the cooling process, which is undesirable. Thus, experiments were repeated in which cooling of the sorbent from 200 °C to the desired adsorption temperature (25°C or 35°C) was in each case carried out in the desired adsorption gas. When the temperature of the sorbent reached the adsorption temperature, the sorbent was held in the adsorption gas for 90 minutes.
ii. Desorption: The adsorption gas was switched to 100 % N_2 gas, and the sorbent was heated to 200 °C. The sorbent was held at this temperature in N_2 gas for 30 min to enable desorption of the adsorbed gas, this completes the first adsorption-desorption cycle.

The adsorption-desorption cycle was carried out 2–3 times to give an indication of the adsorption stability of the sorbents. One long term experiment was also carried out, where the adsorption cycle was repeated 100 loops to study the long-term regeneration ability. The CO_2 working capacity was determined as the difference in the quantity of CO_2 adsorbed during the adsorption and desorption stages of each cycle.[25]

Heat of regeneration: Gray et al.[32] have proposed a simplified energy equation to calculate the regeneration heat for a solid adsorbent based system:

$$Q_r = \Delta H_a + mC_{p,s}\Delta T$$

where Q_r (kJ/mol) is the regeneration heat, ΔH_a (kJ/mol) is the heat of adsorption, m (kg) is the solid mass, $C_{p,s}$ (kJ/kg K) is the solid specific heat capacity and ΔT (K) is the change in temperature.

Cp for the different adsorbents was analysed with a DSC instrument (Mettler Toledo DSC823e) using the Sapphire method. The regeneration heat was measured in the same DSC instrument, and the amount of adsorbed CO_2 was measured in the TGA as described in the previous section.

Evaluation of preliminary techno-economic performance: The preliminary cost estimate has been derived by calculating the operational expenses (OPEX) based on the current estimates of material and energy consumption from laboratory experiments. The high temperature heat (fusion in air, see figure 4) was assumed to be satisfied with direct electrical heating with an efficiency of 95%. The low temperature heat (drying and hydrothermal reaction, see figure 4) was assumed to be satisfied with a heat pump with COP 3, and a heat exchanger efficiency of 55%.[33]

Commodity prices for the OPEX calculations are based on ranges derived, when available, from historic price series:

- Deionized water: Derived from published ranges[34] with a reference commercial price of 0.33 EUR/m³.
- NaOH: Prices obtained from regional quarterly market prices[35] with European prices ranging from 152 to 675 EUR/tonne.
- HCl: Prices obtained from regional quarterly market prices[36] from with prices ranging from 86 to 138 EUR/tonne.
- Electricity: Based on the 10-90th percentile for historic (annual) Swedish electricity prices (22-59 EUR/MWh), according to historical NordPool Spot prices.

Results and discussion

Detailed results from the screening and optimization experiments are available in Appendix 1 and Appendix 2. Here, only the main refined results for selected sorbents are summarized. The CO_2 adsorption performance of the sorbents NZ-1, NZ-2, CA-1, CA-2, PL-1, HS-1, and FA-1 are summarized. The experimental conditions under which these sorbents were developed from the applied feedstocks are presented in Table 1 below.

Table 1. Process conditions and yields for selected sorbents developed from the feedstocks.

Sorbent code	NZ-1	NZ-2	CA-1	CA-2	PL-1	HS-1	FA-1
Feedstock	NZ		NZ		PL	HS	FA
Leaching solvent	1.5 M HCl						
NaOH/Solid residue, mass ratio	1.97	1.97	2.0	2.0	1.5	2.0	2.0
Si/Al, mole ratio	5.4	3.8*	4.9	3.3*	1.1	NA	2.3
Fusion temperature	500 °C						
Fusion retention time	1 hour						
Hydrothermal synthesis (HT) temperature	70 °C						
HT retention time	~18 hours						
Yield (g sorbent/kg feedstock)	652.2	1584.2	654.35	961.43	795.7	157.60	283.2

**Extra Al (in the form of $NaAlO_2$) was added to the solid residue obtained from the leaching step.*

A. Maximum CO_2 working capacity: Figure 5 shows the maximum CO_2 working capacities of the sorbents (NZ-1, NZ-2, CA-1, CA-2, HS-1, PL-1, and FA-1) developed from the applied feedstocks (NZ, CA, HS, PL, and FA). The working capacities were measured at a fixed adsorption temperature of 25 °C and a fixed desorption temperature of 200 °C. Commercial zeolite 13 X is included for comparison. The maximum CO_2 working capacities were measured in 100 % CO_2 gas at 25 °C for 90 minutes. The working capacities of the sorbents increased by at least 3 folds compared to that of the feedstocks from which they were developed. The working capacities (~208–219 g of CO_2 per kg of sorbent) of the sorbents (NZ-1 and NZ-2) developed from natural zeolite (NZ) are closest to that (228.57 g of CO_2 per kg of sorbent) of commercial zeolite 13X. Among the sorbents developed from industrial residues (CA, PL, HS, FA) the working capacities (~129–161 g CO_2 per kg sorbent) of the sorbents (CA-1 and CA-2) developed from CA were the highest. As shown in the Table 1 and explained in the Materials and Method

section, the Si/Al of CA-2 was reduced by adding $NaAlO_2$ during hydrothermal synthesis of the sorbent. Figure 5 shows that the CO_2 working capacity (~161 g of CO_2 per kg of CA-2) of CA-2 which has a lower Si/Al ratio compared to that of CA-1 is higher than the CO_2 working capacity (~129 g of CO_2 per kg of CA-1) of CA-1.This suggest that further process optimization of the synthesis of these sorbents from industrial residues could produce sorbents with CO_2 working capacities that comparable to that of zeolite 13X.

In addition to other factors such as CO_2 selectivity and sorbent degradation, sorbents should have a working capacity of at least 88 g CO_2 per kg of sorbent to be able to compete with the benchmark process for CO_2 separation– chemical absorption with monoethanolamine (MEA).[31, 37]All the developed sorbents but HS-1 and FA-1 meet this minimum working capacity. This makes these sorbents interesting candidates for further development to CO_2 separation. According to Ho et al,[31] a solid sorbent with a CO_2 working capacity of 189.2 g of CO_2 per kg sorbent and a CO_2 selectivity over N_2 of 150 can result in a CO_2 separation cost that is < US$30 per tonne of CO_2 avoided, which is much lower than that (US$49 per tonne of CO_2 avoided) of MEA. The NZ-1 and NZ-2 zeolitic sorbents developed in this work have working capacities that are higher than 189.2 g of CO_2 per kg of sorbent as shown in Figure 5. The higher CO_2 working capacity of CA-2 compared to CA-1 suggests that with further process optimization of the synthesis of these sorbents from industrial residues, sorbents with working capacities close to or even higher than 189. 2 g of CO_2 per kg of sorbent could be obtained.

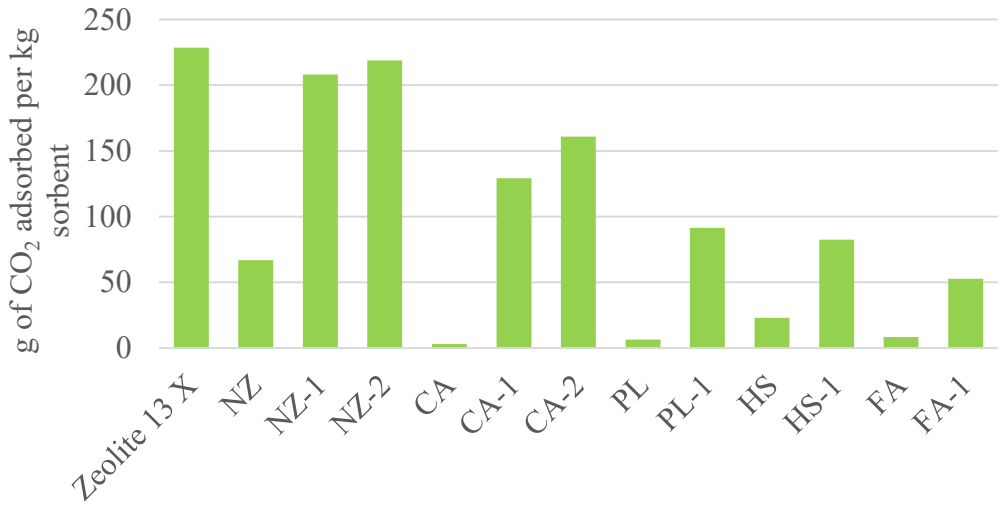

Figure 5. Maximum working capacity of sorbents (NZ-1, NZ-2, CA-1, CA-2, PL-1, HS-1, and FA-1) developed from feedstocks (NZ, CA, HS, PL and FA). Commercial zeolite 13X is included for comparison. The working capacities were measured in 100 % CO_2 gas at adsorption and desorption temperatures of 25°C and 200 °C respectively. The adsorption time was 90 minutes.

The influence of adsorption temperature on the working capacities of some of the sorbents when the desorption temperature was fixed at 200 °C is shown in Figure 6. A slight decrease in the working capacity of each sorbent can be seen as the adsorption temperature was increased from 25°C to 35°C, likely due to the fact that gas adsorption is generally an exothermic process.[38] Similar observation has been reported in literature.[38]

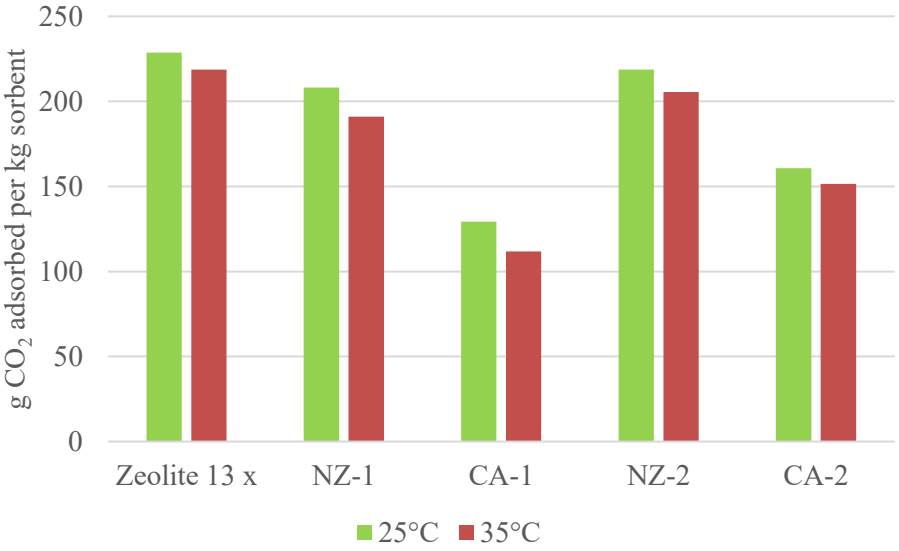

Figure 6. Influence of CO_2 adsorption temperature on the working capacities of the developed sorbents measured in 100 % CO_2 gas at adsorption temperatures of 25°C and 35°C for 90 minutes. The desorption temperature was fixed at 200 °C.

The influence of the desorption temperature on the CO_2 working capacities of some of the sorbents (NZ-2 and CA-2) when the adsorption temperature was fixed at 25°C is shown in Figure 7 below. The working capacities of the sorbents generally increased with desorption temperature. This implies that, for a temperature swing adsorption process, more energy will be needed to raise the sorbents temperature in order to achieve high working capacities.

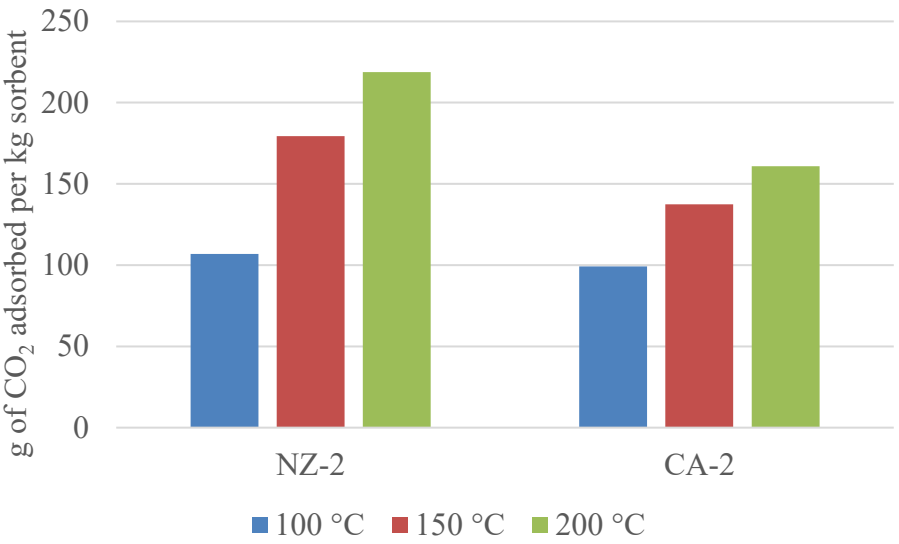

Figure 7. Influence of CO_2 desorption temperature (100 °C, 150 °C, and 200 °C) on the working capacities of the developed sorbents measured in 100 % CO_2 gas at an adsorption temperature of 25 °C.

In an industrial facility for CO_2 separation with solid sorbents, the sorbents operate in continuous adsorption-desorption cycles as shown in Figure 1. To enhance the economic viability of the facility, it is important for the sorbent to be recyclable. Pre-evaluation of the recyclability of the developed sorbents were carried out in a 3 adsorption-desorption cycle. A typical set of 3 adsorption-desorption cycles of CO_2 with the developed sorbents (e.g., CA-2) is shown in Figure 8. During CO_2 adsorption, the mass of the sorbent increases while during desorption, the adsorbed CO_2 is released from the sorbent leading to a decrease in the mass of the sorbent. CO_2 adsorption followed by desorption was virtually stable over the tested 3 cycles.

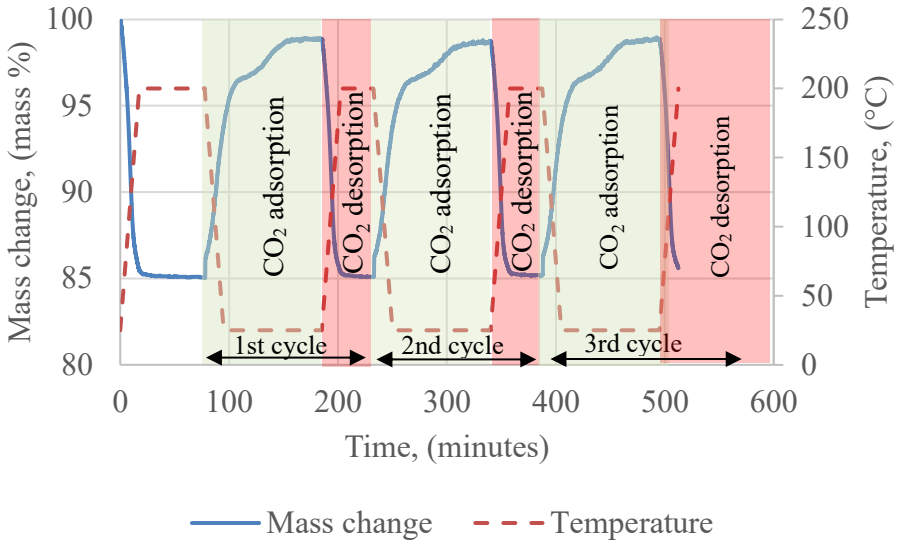

Figure 8. Typical set of 3 adsorption-desorption cycles of CO_2 with the developed sorbents (e.g., CA-2).

To guarantee sorbent stability over time, a long-time experiment with 100 adsorption-desorption cycles in 15% CO_2 was carried out on sorbent PL-1 and the reference Zeolite 13X. The adsorption-desorption graph can be seen in Figure 8. The adsorption capacity for PL-1 dropped by approximately 10% after 10 cycles, 15% after 20 cycles, 18% after 50 cycles and 20% after 100 cycles, compared to the measured capacity during the first cycle. Zeolite 13X did not change at all over the 100 cycles. This can be considered good results, however pure gas mixtures were used in the experiment and a larger drop in capacity can be expected when using real flue gases containing other polluting elements.

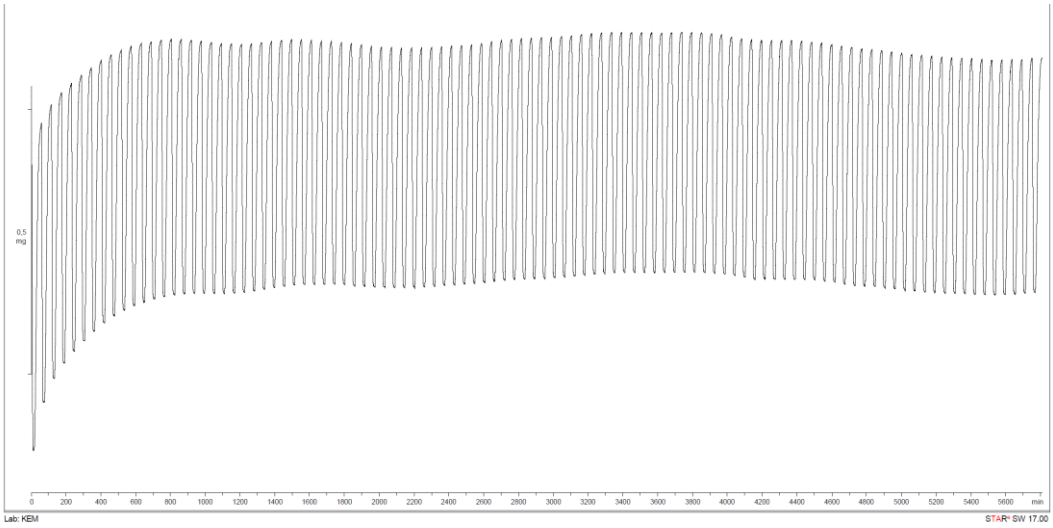

Figure 9. 100 adsorption cycles carried out on sorbent PL-1.

B. CO_2 selectivities of sorbents:

The initial project plan included a stated intention to corroborate the CO_2 capture measured by TGA by selective CO_2 sorption measurements in CO_2/N_2 gas mixtures. These experiments were intended as a complement to the TGA studies to differentiate between N2 and CO_2 uptake in systems where mixed gas streams were investigated. The prediction was that these experiments would have been conducted by adsorption isotherm experiments at varying temperatures and gas compositions similar to experiments performed for surface area measurements. The experiments were going to be conducted at Chalmers but due to instrument malfunction and equipment failure the work could not be conducted as planned.

An alternative experimental plan was devised where CO_2 adsorption in mixed gas systems could be measured by measuring CO_2 release upon sample degasification in a fluidized bed system. This method looked promising on paper but was not practically implementable due to that the material requirements to conduct the experiments outsized our laboratories' zeolite production capacities by roughly an order of magnitude.

Complementary CO_2 sorption selectivity experiments could thus not be conducted as planned during this project. This is unfortunate since the results would have contributed to the understanding of what happens during gas adsorption in the mixed gas systems studied.

C. Gas adsorption in simulated flue gases:

The amount of gas adsorbed by each sorbent in simulated flue gas (15 % CO_2 in N2 gas or 40 % CO_2 in N2 gas) at 25°C for 90 minutes is shown Figure 10. Gas adsorption by the sorbents in 100 % CO_2 and 100 % N_2 is included in the figure for comparison. In the 40 % CO_2 in N2 gas case, the amount of gas adsorbed by the sorbents is either similar to or somewhat smaller than the amount of gas adsorbed in the 100 % CO_2 gas case. In the 15 % CO_2 in N_2 gas case, the amount of gas adsorbed by the sorbents is somewhat similar to that adsorbed by the sorbents in the 100 % CO_2 gas case. The amount of gas (N_2) adsorbed by each sorbent in the 100 % N_2 gas case is similar to the amount of gas (CO_2) adsorbed by the sorbent in the 100 % CO_2 gas case. This suggest that the gas adsorbed by the sorbents in the 40 % CO_2 in N_2 case and the 15 % CO_2 in N_2 case might not be pure CO_2 but a combination of CO_2 and N_2. Establishing the CO_2 selectivities of the sorbents can provide an indication of how selective the sorbents were for CO_2 in the 40 % CO_2 in N_2 and the 15 % CO_2 in N_2 cases.

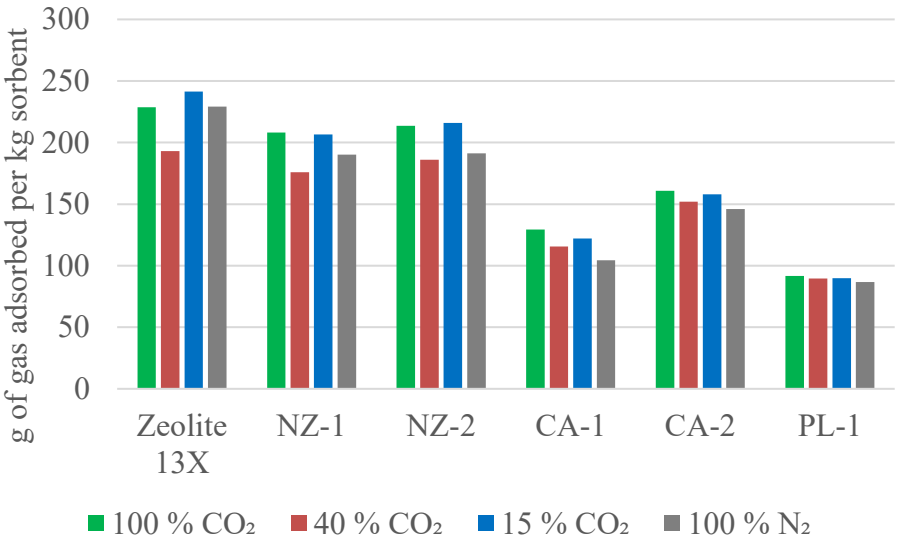

Figure 10. Gas adsorption in various gases measured by 25 °C.

D. Characterization of the sorbents–XRD and BET

Crystallographic, microstructural and specific surface area data was collected to evaluate material properties of the synthesized CO_2 adsorbents evaluated during this work. The crystallographic measurements were conducted by powder X-ray diffraction to identify the presence of known crystalline compounds in the synthesized materials.

The natural zeolite sample was confirmed to be primarily composed mainly of the zeolite clinoptilolite, as had also been confirmed by the supplier. In addition to the clinoptilolite the material also contained some silica, magnesium silicate and sodium silicate

The diffractograms of the synthesized samples NZ-1 and NZ-2 are presented in figures 11 and 12.

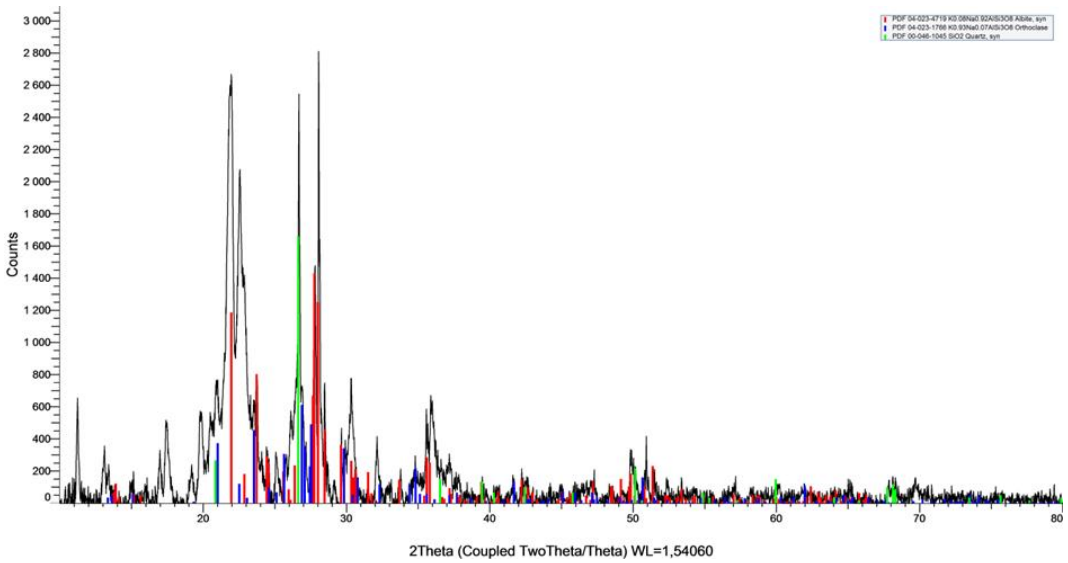

Figure 11. Diffractogram recorded for sample NZ-1

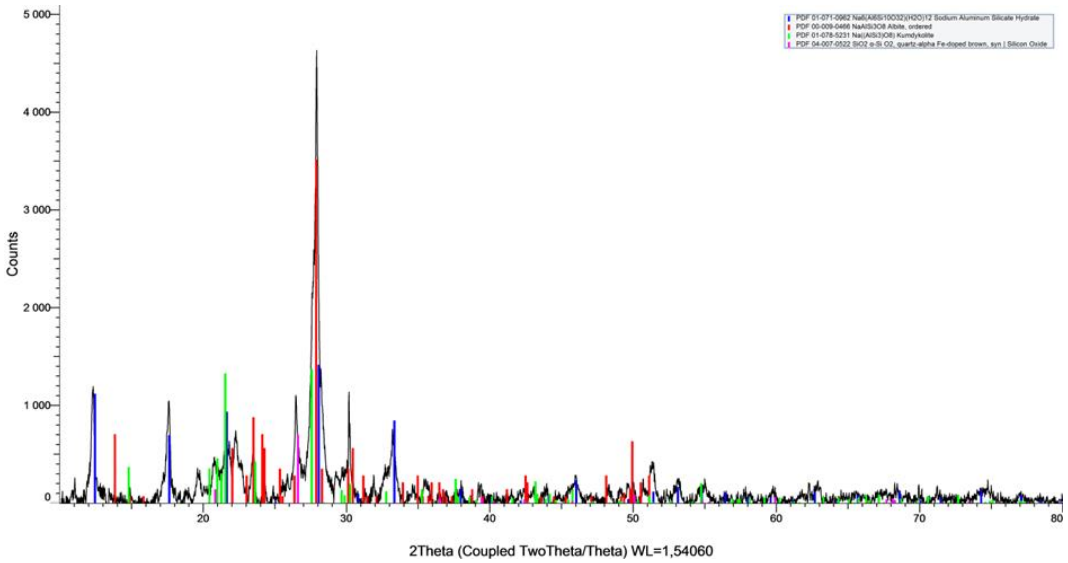

Figure 12. Diffractogram of sample NZ-2.

The crystalline phases identified in NZ-1 and 2 and their specific surface areas are presented in Table 2.

*Table 2. Crystalline phases and associated compound names. The "-" indication is used for identified structures that do not have trivial names. The PDF number relates to the identified compounds catalogue number in the joint **P**owder **D**iffration **F**ile database.*

Sample	Compound	Compound name	PDF number of identified compound	BET surface area (m^2/g)
NZ-1	$K_{0.08}Na_{0.92}AlSi_3O_8$	Albite	04-023-4719	26.3
	$K_{0.93}Na_{0.07}AlSi_3O_8$	Orthoclase	04-023-1766	
	SiO_2	Quartz	00-046-1045	
NZ-2	$Na_6(Al_6Si_{10}O_{32})(H_2O)_{12}$	-	01-071-0962	63.5
	$NaAlSi_3O_8$	Albite, ordered	00-009-0466	
	$Na((AlSi_3)O_8)$	Kumdykolite	01-078-5231	
	SiO_2	Quartz	04-007-0522	

As can be observed in the stoichiometric formulas of the compounds identified several of these compounds are not molecules with exact composition. The diffraction data and database can thus tell us what the closest comparative known compounds are to the ones found in our sample. This does however not guarantee exact stoichiometric compliance with the database. As NZ-1 illustrates we observe two alkali metal aluminum silicates but their chemical composition do not have to match the database reference to the second decimal.

At first look it becomes apparent that no clinoptilolite no longer could be identified in the samples. The alkali fusion and hydrothermal reaction thus changed the material composition so no clinoptilolite can be detected in the sample any longer. Small amounts of SiO_2 was detected both in the treated samples and in the untreated zeolite sample, implying the SiO_2 might remain fairly inert at tested synthesis conditions.

The presence of potassium in the NZ-1 sample should be viewed somewhat skeptically since NaOH and not KOH was added during zeolite synthesis. Since the crystallographic interpretation of data is made by database comparison, the reported structure is that of the closest matching compound structure. What is matched is thus structure and not composition. Three similar alkali metal aluminum silicates were detected in NZ-1 and NZ-2, $K_{0.08}Na_{0.92}AlSi_3O_8$, $K_{0.93}Na_{0.07}AlSi_3O_8$ and $NaAlSi_3O_8$. These compounds are very similar with the difference that in two of them various degree of Na have been substituted with K, and K is a larger ion than Na in any give coordination number[39]. What is observed in sample NZ-1 is thus likely an $NaAlSi_3O_8$ with a slight lattice distortion shifting the diffraction peaks towards something looking like a material containing

potassium substitution due to a lattice expansion in the $NaAlSi_3O_8$, likely due to synthesis conditions being a bit too short for the $NaAlSi_3O_8$ to fully form in a non-strained state.

The NZ-1 and NZ-2 sample possessed significantly different specific surface area but similar crystalline phases, the difference being NZ-2 contained also a lower Si/Al ratio aluminum silicate, $Na_6(Al_6Si_{10}O_{32})(H_2O)_{12}$, which would imply this compound contributes strongly to the specific surface area of the sample. NZ-1 and NZ-2 performed similar in CO_2 adsorption during TGA experiments, leading to the interpretation that specific surface area, important as it might be, is less influential on gas adsorption properties than the composition of the aluminum silicates present in the material.

The untreated natural zeolite displayed a lower CO_2 capture potential than the treated materials NZ-1 and NZ-2. Also, NZ-1 and NZ-2 performed very similar in CO_2 adsorption capacity. This points towards that the higher Si/Al molar ratio aluminum silicates present in NZ-1 and NZ-2 (Si/Al = 2.67) are more beneficial towards CO_2 capture than the lower Si/Al molar ratio aluminum silicates present in the clinoptilolite and NZ-2 (Si/Al molar ratios of 1.36 and 1.67 respectively).

The cyclone ash (CA) displayed virtually no CO_2 capture potential prior to alkali fusion and hydrothermal reaction. The diffractograms recorded for samples CA-1 and CA-2 are presented in figures 13 and 14.

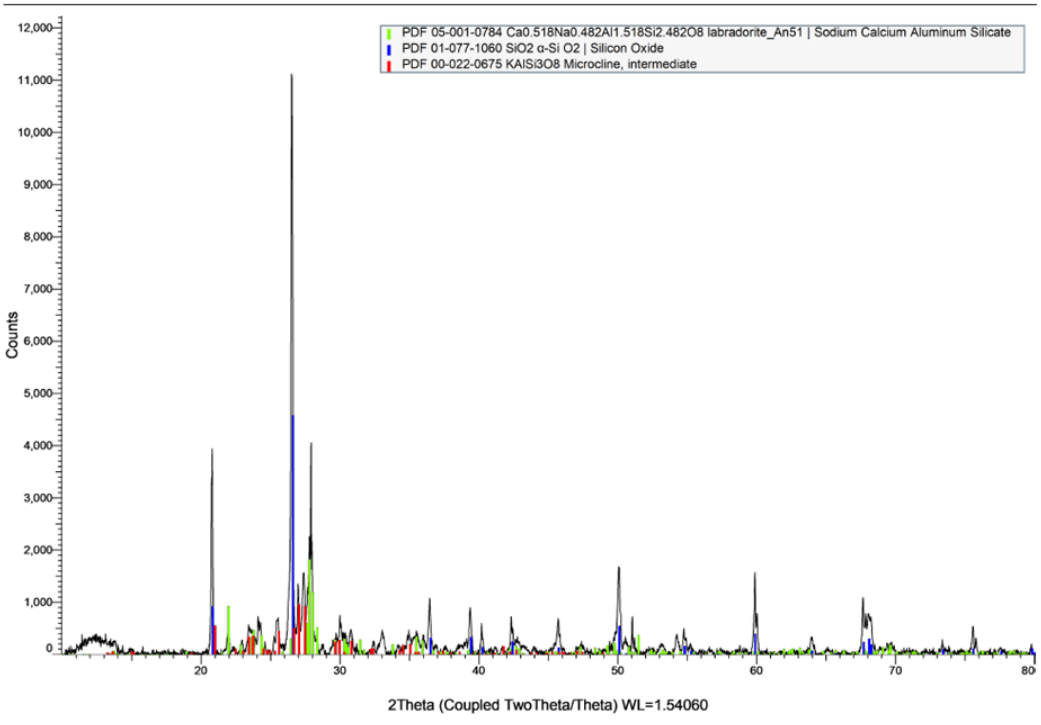

Figure 13. Diffractogram of sample CA-1.

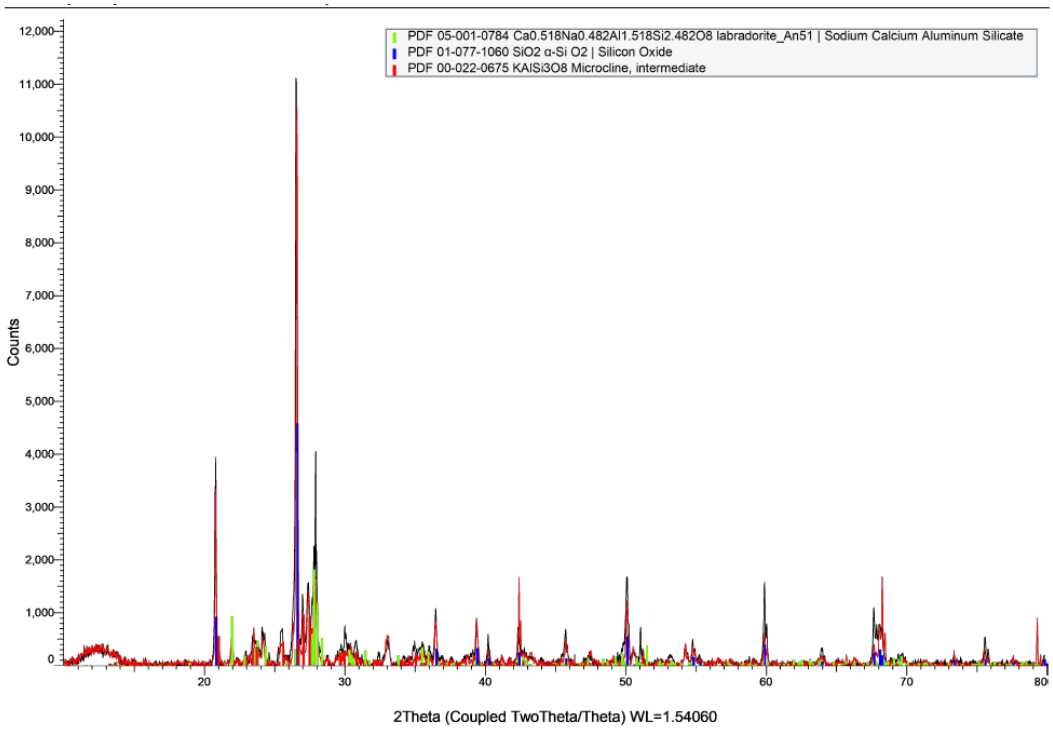

Figure 14. Comparative diffractogram between samples CA-1 and CA-2.

As can be observed in figure 14, the plotted diffractograms of CA-1 and CA-2 more or less completely superimpose on top one another, proving that the same crystalline compounds exist in both materials, although possibly in slightly different concentrations. Summarized data for identified crystalline phases and specific surface areas are presented in Table 3.

Table 3. Crystalline phases measured in samples CA-1 and CA-2

Sample	Compound	Compound name	PDF number of identified compound	BET surface area (m^2/g)
CA1	$Ca_{0.518}Na_{0.482}Al_{1.518}Si_{2.482}O_8$	Labradorite	05-001-0784	7.3
	SiO_2	α-SiO2	01-077-1060	
	$KAlSi_3O_8$	Microcline	00-022-0675	
CA2	$Ca_{0.518}Na_{0.482}Al_{1.518}Si_{2.482}O_8$	Labradorite	05-001-0784	31.8
	SiO_2	α-SiO2	01-077-1060	
	$KAlSi_3O_8$	Microcline	00-022-0675	

Samples CA-1 and CA-2 appears to be very similar with respect to their compositions and there are also some similarities to NZ-1 and NZ-2. Just as in those samples a separate SiO_2 phase can be detected and presence of an $AlSi_3O_8$ material, charge balanced by either K, Na or a mix of them exist in all four materials. There is some potassium in both the untreated cyclone ash and natural zeolite but as in the NZ samples one can suspect that the $KAlSi_3O_8$ at least partially should contain also some Na in the structure due to its higher concentration in the reaction mixtures during synthesis. A common feature of the produced CO_2 adsorbents is that they seem to contain a $(Na/K)AlSi_3O_8$ type of material that thus could be the material responsible for the increased CO_2 capture potential.

One differing property between CA-1 and CA-2 is the specific surface area of the materials. As of current there is no good explanation to why two materials, synthesized by similar conditions and appearing to contain the same compounds ended up with so varying specific surface area. But there seems to be an effect of the additional surface area since CA-2 displayed a higher CO_2 capture potential in the TGA experiment, even if the performance improvement was limited in this respect.

The industrial slag product Petrit L (PL) demonstrated significantly increased CO_2 capture properties once processed compared to the provided raw material. The diffractogram of PL-1 is presented in figure 15.

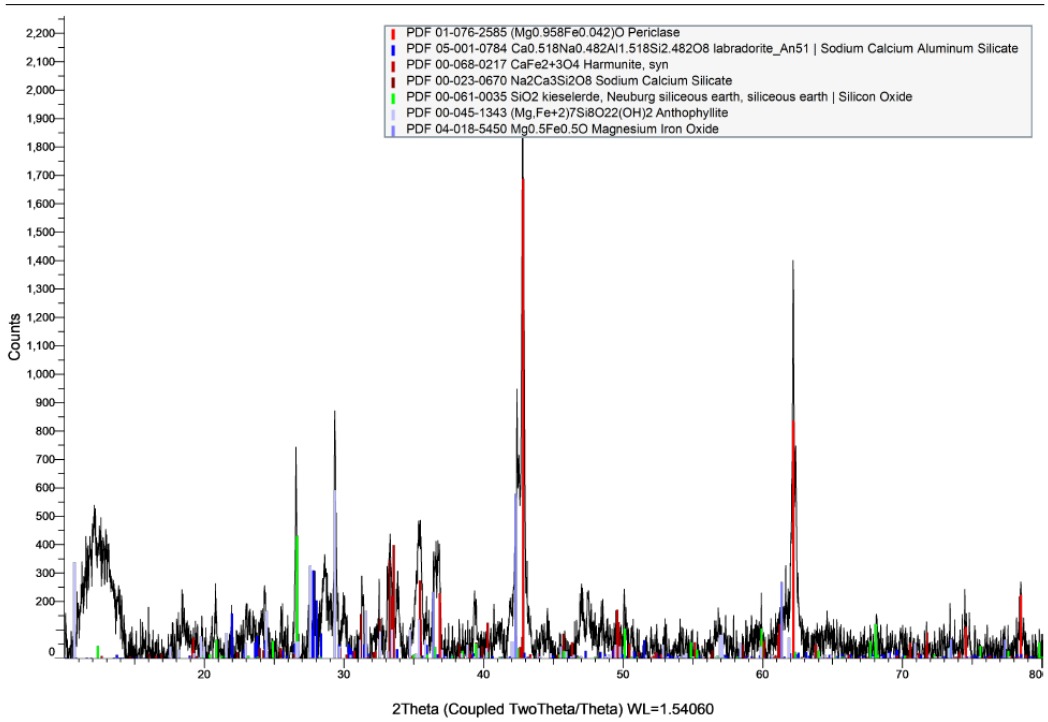

Figure 15. Diffractogram of PL-1.

The first thing to notice is the significantly worse data quality compared to previous diffractograms, the peak intensities recorded differ by almost an order of

magnitude in relation to diffraction peaks observed in previous materials. This makes phase identification more difficult and the data quality is influenced by the composition of the sample. The PL slag is an iron-based slag and the Cu-Kα radiation used to perform the diffraction measurements are absorbed and reemitted by the iron in the sample. This causes high noise levels in the samples and contribute to decreased data quality. Table 4 presents the phases identified in the sample but the results should be viewed as somewhat more uncertain than previous phase identifications.

Table 4. Identified crystalline phases in sample PL-1.

Sample	Compound	Compound name	PDF number of identified compound	BET surface area (m^2/g)
PL1	$(Mg_{0.958}Fe_{0.042})O$	Periclase	01-076-2585	43.5
	$Ca_{0.518}Na_{0.482}Al_{1.518}Si_{2.482}O_8$	Labradorite	05-001-0784	
	$CaFe_2O_4$	Harmunite	00-068-0217	
	$Na_2Ca_3Si_2O_8$	-	00-023-0670	
	SiO_2	Kieselerde	00-061-0035	
	$(Mg,Fe)_7Si_8O_{22}(OH)_2$	Anthophyllite	00-045-1343	

The starting material is known to contain both Ca, Mg and Fe so finding calcium-iron and magnesium-iron compounds in the treated material is expected. Due to the number of possible crystalline phases encountered in the material it is hard to identify which actually carries the more significant influence on the CO_2 capture properties. Although there seems to be Labradorite in the sample just as in CA-1 and CA-2. So, either the Labradorite is also responsible for part of the CO_2 capture observed in CA-1 and CA-2 or it is one of the other silicates in PL-1 that binds CO_2. Since iron, magnesium, calcium and silicon were all present in PL before sample treatment and very little CO_2 capture was observed upon testing it does however imply that the added aluminum during synthesis contributed to forming the compound capturing CO_2 and that would be the Labradorite. Too strong conclusions should however not be drawn from the diffraction data due to its lower quality in the PL samples.

E. Heat of regeneration

The calculated energy required to generate the adsorbents in a TSA cycle is shown in Table 5. All values are around or below 2 GJ/tonne CO_2 which was the target. Adsorbent PL1 has the lowest energy consumption but also the lowest working capacity.

Table 5: Regeneration heat for some of the produced adsorbents.

Adsorbent	Regeneration heat (GJ/tonne CO_2)
Zeolite 13X	2,08
PL1	0,87
CA2	1,47
NZ2	1,22

F. Preliminary economic analysis.

The estimated mass- and energy balance from the laboratory measurements and based on the assumptions regarding heating sources are shown below in Figure 16.

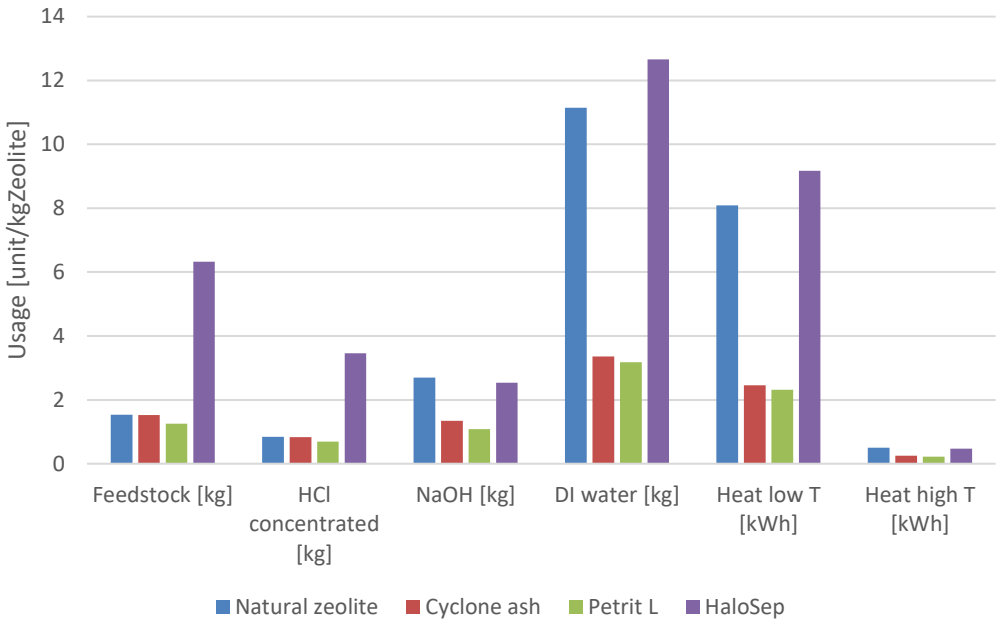

Figure 169. Usage of chemicals, deionized water, and energy for the production of one kg of zeolites. Chemical consumption is shown for concentrated chemicals.

The resulting mass and energy balance shown in Figure 17 shows that the feedstock HaloSep is an outlier in terms of usage of feedstock usage for the production of the zeolites. The high feedstock usage results in the corresponding high usage of the other commodities as more chemicals are needed to leech the feedstock, and subsequently more DI water is needed for rinsing, and more energy needed for the drying.

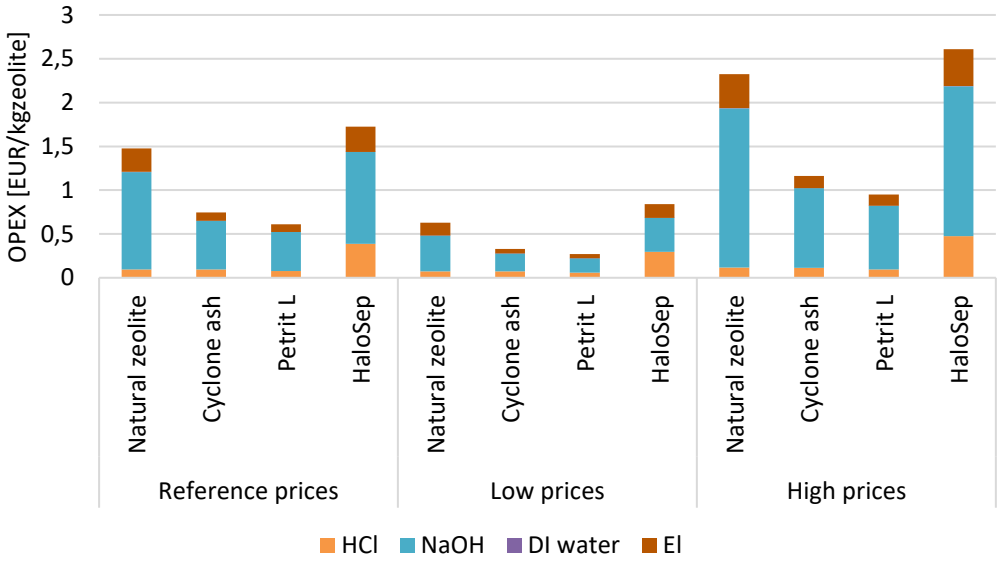

Figure 1710. OPEX production cost related to energy, chemicals, and water usage.

The figure presents the OPEX costs for the production of a material under different price scenarios: reference prices, low prices, and high prices, showing for all feedstocks and price scenarios a OPEX range from 0.3 – 2.6 EUR/kg of produced zeolite. The use of NaOH and HCl are the primary cost driver for the process. The OPEX shows favorable results for Cyclone ash and Petrit L feedstocks which show a cost of 0.7 EUR/kg and 0.6 EUR/kg of produced zeolites, respectively, for the reference prices scenario. Simultaneously, the HaloSep feedstock shows a significantly higher OPEX, suggesting that selecting appropriate feedstocks can significantly reduce the overall production costs, making the process more economically viable. These OPEX figures should be expected to be possible to be reduced with optimization of the chemical usage in relation to the specific feedstock, however, several additional cost components have not been included in this analysis, where the major are assumed to be:

- Feedstock handling cost: Expenses related to the handling, storage, and transportation of raw materials.
- Income from use of waste – Cost of depositing residue: Potential income from utilizing waste by-products and the associated costs of disposing of any residual waste.
- Capital cost: Initial investment required for equipment, facilities, and infrastructure necessary for the production process.
- Resulting performance in CO_2 capture: The performance of the implemented process in relation to CO_2 capture, especially when compared to using commercial Zeolite 13x or amine-based CO_2 capture methods.

These costs could significantly impact the overall techno-economic assessment of the technology and need to be considered for a more comprehensive evaluation of the future commercial-scale performance for the production of synthetic zeolites from waste material.

Conclusions

It is possible to produce zeolites from industrial residues using the method described in this report. The zeolites have a CO_2 adsorption capacity that is higher than the minimum required to make them a viable alternative to current commercial products. The energy consumption for regeneration is significantly lower than for the MEA technology, and it was shown that with clean simulation gas it was possible to repeat the adsorption-desorption cycle 100 times without loosing much of the working capacity.

OPEX for producing the zeolites varies significantly across different feedstocks and price scenarios, ranging from 0.3 to 2.6 EUR/kg. NaOH and HCl are the primary cost drivers, and feedstocks like Cyclone ash and Petrit L show more favourable OPEX results at 0.7 EUR/kg and 0.6 EUR/kg respectively under reference price conditions. The feedstock used in the production of the zeolites plays a significant role in the resulting techno-economic performance. Poor feedstock selection will lead to high consumption of chemicals, deionized water, and energy, which in turn raises the overall production costs. While the current OPEX figures are promising, especially for certain feedstocks, there is potential for further reduction through the optimisation of chemical usage. However, additional cost factors such as feedstock handling, income from waste utilisation, capital costs, and CO_2 capture performance are not accounted for in this analysis and could significantly affect the techno-economic viability of the process.

Appendix

- Appendix 1: Utveckling av zeoliter för CO_2-avskiljning; Master thesis by Andreas Bengtsson.
- Appendix 2: Development of low-cost zeolites for cost-efficient CO_2 capture; Master's thesis by Adriana Mateu Alcácer.

References

1. Cementa. "Färdplan cement för ett klimatneutralt betongbyggande." https://www.cementa.se/sv/fardplancement (accessed.
2. Jernkontoret. "Klimatfärdplan för en fossilfri och konkurrenskraftig stålindustri i Sverige." https://www.jernkontoret.se/sv/vision-2050/klimatfardplan/ (accessed.
3. S. Budinis, S. Krevor, N. M. Dowell, N. Brandon, and A. Hawkes, *Energy Strategy Reviews,* vol. 22, pp. 61-81, 2018/11/01/ 2018, doi: https://doi.org/10.1016/j.esr.2018.08.003.
4. S. Ó. Garðarsdóttir, F. Normann, R. Skagestad, and F. Johnsson, *International Journal of Greenhouse Gas Control,* vol. 76, pp. 111-124, 2018/09/01/ 2018, doi: https://doi.org/10.1016/j.ijggc.2018.06.022.
5. The European Energy Exchange (**EEX**) https://www.eex.com.
6. D. Y. C. Leung, G. Caramanna, and M. M. Maroto-Valer, *Renewable and Sustainable Energy Reviews,* vol. 39, pp. 426-443, 2014/11/01/ 2014, doi: https://doi.org/10.1016/j.rser.2014.07.093.
7. N. Susarla *et al.*, *Chemical Engineering Research and Design,* vol. 102, pp. 354-367, 2015/10/01/ 2015, doi: https://doi.org/10.1016/j.cherd.2015.06.033.
8. M. Songolzadeh, M. Soleimani, M. Takht Ravanchi, and R. Songolzadeh, *The Scientific World Journal,* vol. 2014, p. 828131, 2014/02/17 2014, doi: 10.1155/2014/828131.
9. K. A. Fayemiwo *et al.*, *Chemical Engineering Journal,* vol. 334, pp. 2004-2013, 2018/02/15/ 2018, doi: https://doi.org/10.1016/j.cej.2017.11.106.
10. Y. Wang, L. Zhao, A. Otto, M. Robinius, and D. Stolten, *Energy Procedia,* vol. 114, pp. 650-665, 2017/07/01/ 2017, doi: https://doi.org/10.1016/j.egypro.2017.03.1209.
11. B. Belaissaoui and E. Favre, *Oil Gas Sci. Technol. – Rev. IFP Energies nouvelles,* vol. 69, no. 6, pp. 1005-1020, 2014. [Online]. Available: https://doi.org/10.2516/ogst/2013163.
12. R. M. Cuéllar-Franca and A. Azapagic, *Journal of CO2 Utilization,* vol. 9, pp. 82-102, 2015/03/01/ 2015, doi: https://doi.org/10.1016/j.jcou.2014.12.001.
13. Q. Al-Naddaf, S. Lawson, A. A. Rownaghi, and F. Rezaei, *AIChE Journal,* vol. 66, no. 9, p. e16297, 2020, doi: https://doi.org/10.1002/aic.16297.
14. S. Bergström, "Koldioxidavskiljning på ett biobränsleeldat kraftvärmeverk–Simulering av två avskiljningstekniker vid Karlstad Energis kraftvärmeverk, Heden 3," Karlstads universitet, 2020.
15. E. I. Koytsoumpa, C. Bergins, and E. Kakaras, *The Journal of Supercritical Fluids,* vol. 132, pp. 3-16, 2018/02/01/ 2018, doi: https://doi.org/10.1016/j.supflu.2017.07.029.
16. P. Rzepka *et al.*, *The Journal of Physical Chemistry C,* vol. 122, no. 30, pp. 17211-17220, 2018/08/02 2018, doi: 10.1021/acs.jpcc.8b03899.
17. M. Bui *et al.*, *Energy & Environmental Science,* 10.1039/C7EE02342A vol. 11, no. 5, pp. 1062-1176, 2018, doi: 10.1039/C7EE02342A.

18. M. Oschatz and M. Antonietti, *Energy & Environmental Science,* 10.1039/C7EE02110K vol. 11, no. 1, pp. 57-70, 2018, doi: 10.1039/C7EE02110K.
19. S. Krishnamurthy *et al.*, *AIChE Journal,* vol. 60, no. 5, pp. 1830-1842, 2014, doi: https://doi.org/10.1002/aic.14435.
20. K. Guojun, S. Haichen, and Y. Pengfei, *Materials,* vol. 12, no. 13, p. 3895, 2019.
21. S. K. Wahono, J. Stalin, J. Addai-Mensah, W. Skinner, A. Vinu, and K. Vasilev, *Microporous and Mesoporous Materials,* vol. 294, p. 109871, 2020/03/01/ 2020, doi: https://doi.org/10.1016/j.micromeso.2019.109871.
22. Z. Zhang, Y. Xiao, B. Wang, Q. Sun, and H. Liu, *Energy Procedia,* vol. 114, pp. 2537-2544, 2017/07/01/ 2017, doi: https://doi.org/10.1016/j.egypro.2017.08.036.
23. M. M. Yassin, S. Biti, W. Afzal, and C. Fernández Martín, *Journal of Environmental Chemical Engineering,* vol. 9, no. 6, p. 106835, 2021/12/01/ 2021, doi: https://doi.org/10.1016/j.jece.2021.106835.
24. M. Erguvan and S. Amini, *Carbon Capture Science & Technology,* vol. 11, p. 100189, 2024/06/01/ 2024, doi: https://doi.org/10.1016/j.ccst.2024.100189.
25. F. Raganati, R. Chirone, and P. Ammendola, *Industrial & Engineering Chemistry Research,* vol. 59, no. 8, pp. 3593-3605, 2020/02/26 2020, doi: 10.1021/acs.iecr.9b04901.
26. C.-H. Yu, C.-H. Huang, and C.-S. Tan, *Aerosol and Air Quality Research,* vol. 12, no. 5, pp. 745-769, 2012, doi: 10.4209/aaqr.2012.05.0132.
27. R. Zhao *et al.*, *Energy,* vol. 137, pp. 495-509, 2017/10/15/ 2017, doi: https://doi.org/10.1016/j.energy.2017.01.158.
28. N. Jiang *et al.*, *Journal of CO2 Utilization,* vol. 35, pp. 153-168, 2020/01/01/ 2020, doi: https://doi.org/10.1016/j.jcou.2019.09.012.
29. P. A. Saenz Cavazos, E. Hunter-Sellars, P. Iacomi, S. R. McIntyre, D. Danaci, and D. R. Williams, (in English), *Frontiers in Energy Research,* Review vol. 11, 2023-July-27 2023, doi: 10.3389/fenrg.2023.1167043.
30. F. Raganati, F. Miccio, and P. Ammendola, *Energy & Fuels,* vol. 35, no. 16, pp. 12845-12868, 2021/08/19 2021, doi: 10.1021/acs.energyfuels.1c01618.
31. M. T. Ho, G. W. Allinson, and D. E. Wiley, *Industrial & Engineering Chemistry Research,* vol. 47, no. 14, pp. 4883-4890, 2008/07/01 2008, doi: 10.1021/ie070831e.
32. Gray ML, Hoffman JS, Hreha DC, et al. Parametric study of solid amine sorbents for the capture of carbon dioxide. Energy Fuels 2009;23:4840–4.
33. Delele MA, Weigler F, Mellmann J. Advances in the Application of a Rotary Dryer for Drying of Agricultural Products: A Review. Drying Technology 2015;33:541–58. https://doi.org/10.1080/07373937.2014.958498.
34. Liu X, Shanbhag S, Bartholomew TV, Whitacre JF, Mauter MS. Cost Comparison of Capacitive Deionization and Reverse Osmosis for Brackish Water Desalination. ACS EST Eng 2021;1:261–73. https://doi.org/10.1021/acsestengg.0c00094.

35. Chemanalyst. Caustic Soda Prices, Price, Pricing, Monitor | ChemAnalyst 2023. https://www.chemanalyst.com/Pricing-data/caustic-soda-3.
36. Chemanalyst. Hydrochloric Acid Prices, Price, Pricing, Monitor | ChemAnalyst 2023. https://www.chemanalyst.com/Pricing-data/hydrochloric-acid-61.
37. H. E. Holmes, R. P. Lively, and M. J. Realff, *JACS Au,* vol. 1, no. 6, pp. 795-806, 2021/06/28 2021, doi: 10.1021/jacsau.0c00127.
38. T. F. d. Aquino *et al.*, *Fuel,* vol. 276, p. 118143, 2020/09/15/ 2020, doi: https://doi.org/10.1016/j.fuel.2020.118143.
39. R.D., Shannon, *Acta Crystallographica,* vol 32, 1976, doi: https://doi.org/10.1107/S0567739476001551